

# Analytical assessment of coupled influences of surrounding rock reinforcement and deformation release on tunnel response

Su Qin<sup>1,2a</sup>, Kui Wu<sup>1,2b</sup> and Zhushan Shao<sup>\*1,2</sup>

<sup>1</sup>*Xi'an University of Architecture and Technology, Xi'an 710055, China*

<sup>2</sup>*Shaanxi Key Lab of Geotechnical and Underground Space Engineering (XAUAT), Xi'an 710055, China*

*(Received May 10, 2021, Revised June 16, 2021, Accepted September 14, 2021)*

**Abstract.** Attempt has been proved to be effective that surrounding rock reinforcement is emphasized simultaneously considering displacement release in weak rock tunnels. In this study, the calculation formulas for mechanical parameters of bolt-reinforced rocks are provided using the homogenization method and the supporting characteristic curve is divided into three stages with proposing the corresponding stiffness equations. The mechanical model for bolted-reinforced rock-yielding supports interaction is then established and coupled solutions for displacements and stresses around tunnels considering bolt reinforcement and yielding effects are provided. Furthermore, parametric investigations on the influences of rockbolts and yielding supports are carried out. Results show that (1) rock displacement gradually decreases as the rockbolt length increases. However, when rockbolt length becomes large enough, the further improvement of rock displacement will not be obvious by still increasing their length. (2) Both rock displacement and plastic zone of tunnel decrease with the increase of rockbolt radius. There exists the highest utilization of rockbolts corresponding to a certain rockbolt radius. (3) Also, the rock displacement and plastic zone of tunnel decrease as installation density of rockbolts including circumferential space and longitudinal space increases. Under the condition prescribed, this decreasing trend becomes sharper and the improvement is more evident. (4) Larger yielding displacement or stiffness parameter leads to smaller support pressure, but greater plastic radius of tunnel. The optimal yielding displacement and stiffness parameters need to be determined through a comprehensive investigation combining rock properties, support characteristics and tunnel design requirements.

**Keywords:** analytical solution; deep tunnel; novel supporting concept; rockbolt reinforcement; yielding supports

## 1. Introduction

With the rapid development of tunnelling technology, many difficult tunnels had been built throughout the world (Kimura *et al.* 1987, Barla *et al.* 2011, Ranjbarnia *et al.* 2020). Statistics show that large deformation was one of the most common problems occurring in weak rock tunnels at great depth during construction, accompanied by support failure (Chu *et al.* 2021a, b, Fan *et al.* 2020, 2021, Sun *et al.* 2020, 2021). Actually, a good solution for deep underground excavation in weak rocks is that rock masses are reinforced inward and support has the capacity of accommodating rock deformations without being damaged (Cantieni and Anagnostou 2009).

Basically, rockbolts have been widely used to stabilize underground openings by improving the rock mechanical performance (Fahimifar and Ranjbarnia 2009, Zhao *et al.* 2021). According to the previous studies, the rock bolting

effects can be grouped as the ground sewing, geomechanical properties improving (both cohesion and

frictional angle) of rock masses, and adding internal as a confining pressure within a broken rock masses (Fahimifar and Ranjbarnia 2009). In order to better design the rockbolts, Cai *et al.* (2015) presented an interaction model to describe the interaction behaviors of rockbolts and rocks. Cui *et al.* (2019) provided a simplified procedure for analysing the interaction between bolts and rocks for circular tunnels. Bobet (2009) derived elastic solution for bolted tunnel. Using the homogenization method, convergence-confinement predictions for bolt-supported tunnels were also put forward (Bernaud *et al.* 1995, Wong *et al.* 2006, Osgoui and Oreste 2007, Yan *et al.* 2017).

Unfortunately, although rockbolts have been installed in tunnels, original stiff supports sometimes still failed to resist large deformations (Eftekhari and Aalianvari 2019, Wu *et al.* 2021a, b, 2022a). Recently, based on the deeper understanding of deformation mechanisms of weak rock tunnels at great depth, yielding supports have been attracting more and more research interests. The term of “yielding supports” refers as the supports having the capacity of accommodating rock deformations, and the idea behind them is that the rock deformation pressure acting on supports will decrease by allowing the rocks to deform (Wu and Shao 2019a, 2019b). In Enasan tunnel II (Kimura *et al.* 1987), Yacambú-Quibor tunnel (Hoek and Guevara 2009), Saint Martin La Porte access adit (Barla *et al.* 2011), Dongtan coal mine (Tan *et al.* 2017) *et al.*, the application of the support system of “rockbolts and yielding supports”

\*Corresponding author, Professor, Ph.D.

E-mail: shaozhushan@xauat.edu.cn

<sup>a</sup>Ph.D. Student

<sup>b</sup>Lecturer, Ph.D.

<sup>c</sup>Professor, Ph.D.

have successfully addressed the support failure problem induced by large deformations. Generally, the yielding supports, based on the yielding method, can be classified into two groups: the radial and tangential (Cantiemi and Anagnostou 2009). Radially yielding supports allow rock deformations to develop outside the liner extrados by installing a compressible layer between the rocks and the stiff liner. Tangentially yielding supports are able to accommodate a certain reduction in their circumstances through a structural detailing of liner or adding yielding elements into liner. Moritz (2011) have attempted to summarize the types and mechanical properties of tangential yielding liner. Radončić *et al.* (2009) investigated the tunnel response supported by different ductile lining systems. Hoek and Guevara (2009) successfully overcame the squeezing large deformation occurring in the Yacambú-Quibor tunnel using the yielding supports. Öge (2021) discussed the energy absorption of flexible supports in a mine roadway. Wu and Shao (2019) proposed the analytical solutions for stresses and displacements around tunnels where a compressible layer is used. Wu *et al.* (2020a, b, 2022b) proposed an analytical design approach for tangential yielding liner and determined its stiffness calculation method. It is generally accepted that theoretical solutions are very important for underground excavation problems, helping clarify the mechanisms of generation and change of stresses and displacements around tunnels and achieve a better understanding of how final solutions are affected by parameters included (Exadaktylos and Stavropoulou 2002; Brichall *et al.* 2012; Kargar *et al.* 2014). However, up to now there has been very little literature on analytical solution for yielding supports. Even, some solutions were obtained based on the assumption of that the support pressure is the constant. In this condition, it is necessary to conduct a theoretical investigation on the mechanical behaviour of tunnels supported by yielding supports.

In this paper, the theoretical investigation on the mechanical behaviour of a lined tunnel is carried out, considering the rockbolt reinforcement and yielding effects. Furthermore, a parametric study on the influence of parameters of rockbolts and yielding supports is performed. The results in this paper can provide useful guidance for tunnel design.

## 2. Solution

### 2.1 General consideration

This problem deals with a circular tunnel supported by rockbolts and yielding supports within elasto-plastic geomaterials. The tunnel is located at such a great depth compared with tunnel dimension that the problem is considered a reinforced hole in an infinite plane, subjected to a uniform stress state at infinity (Kargar *et al.* 2014). Original rock masses, bolted rock masses and supports are assumed as isotropic and homogeneous materials. Original and bolted rock masses are both subjected to Mohr-Coulomb strength criteria (Yan *et al.* 2017) and the supports behave linearly elastic before failure. The length of

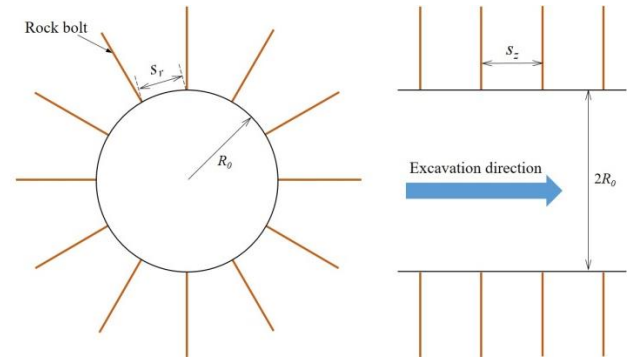


Fig. 1 Illustration of bolt-reinforced tunnel

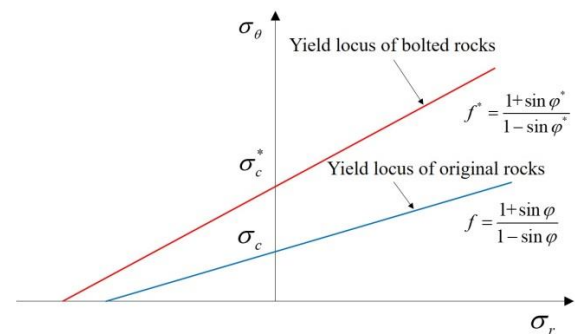


Fig. 2 Yield locus of original and bolted rocks in principal-stress coordinate

rockbolts is assumed to be larger than the plastic radius of tunnel. It is also supposed that there is not any support delay after tunnel excavation.

### 2.2 Mechanical parameters of bolted rocks

Using the homogenization method the bolted rock masses are considered as isotropic and homogeneous composite geomaterials (Bernaud *et al.* 1995, Wong *et al.* 2006, Osgoui and Oreste 2007, Yan *et al.* 2017). Based on the equivalent stiffness approach the equivalent Young's modulus of the bolted rock masses can be calculated as

$$E^* A^* = E_1 A_1 + E_2 A_2 \quad (1)$$

where  $E^*$  and  $A^*$  denote the Young's modulus and area of bolted rock masses, respectively.  $E_1$  and  $A_1$  are the Young's modulus and area of original rock masses, respectively.  $E_2$  and  $A_2$  represent the Young's modulus and area of rockbolts, respectively.

The arrangement of rockbolts in tunnels is shown in Fig. 1. Substituting the rockbolt parameters into the Eq. (1) yields the Young's modulus of bolted rock masses as follows

$$E^* = \frac{E_2 \pi r_b^2 + E_1 (s_r s_z - \pi r_b^2)}{s_r s_z} \quad (2)$$

where  $s_r$  and  $s_z$  denote the circumferential and longitudinal spaces of rockbolts, respectively.  $r_b$  is the radius of rockbolts.

In polar coordinate system the Mohr-Coulomb strength criteria can be written as

$$\sigma_{\theta} = \frac{1 + \sin \varphi}{1 - \sin \varphi} \sigma_r + \sigma_c \quad (3)$$

where  $\sigma_r$  and  $\sigma_{\theta}$  represent the radial and tangential stresses, respectively.  $c$  and  $\varphi$  are cohesion and internal friction angle of geomaterial, respectively. And  $\sigma_c$  can be given by

$$\sigma_c = \frac{2c \cos \varphi}{1 - \sin \varphi} \quad (4)$$

As shown in Fig. 2, the yield locus of original rocks  $f$  in principal-stress coordinate is plotted. On account of reinforcement of rockbolts, the yield locus of bolted rocks will change into  $f^*$ .

The relationship between two yield loci of original and bolted rocks can be written as

$$f^* = (1 + \alpha) f \quad (5)$$

where  $\alpha$  denotes the rockbolt density factor (Indraratna and Kaiser 1990) and can be expressed as

$$\alpha = \frac{2\pi r_b \tan \varphi}{s_r s_c} \quad (6)$$

Then  $\sigma_c^*$  can be given by

$$\sigma_c^* = (1 + \alpha) \sigma_c \quad (7)$$

Combining the Eqs. (5) and (7), the relationships of cohesion and internal friction angle of original and bolted rock masses can be given by

$$\frac{2c^* \cos \varphi^*}{1 - \sin \varphi^*} = (1 + \alpha) \frac{2c \cos \varphi}{1 - \sin \varphi} \quad (8)$$

$$\frac{1 + \sin \varphi^*}{1 - \sin \varphi^*} = (1 + \alpha) \frac{1 + \sin \varphi}{1 - \sin \varphi} \quad (9)$$

Then by solving the Eqs. (8) and (9), the cohesion and internal friction angle of bolted rock masses can be expressed by those of original rock masses as

$$c^* = \frac{c(1 + \alpha)(1 - \sin \varphi^*) \cos \varphi}{(1 - \sin \varphi) \cos \varphi^*} \quad (10)$$

$$\varphi^* = \arcsin \left[ \frac{(1 + \sin \varphi) \alpha + 2 \sin \varphi}{(1 + \sin \varphi) \alpha + 2} \right] \quad (11)$$

### 2.3 Supporting equations for yielding supports

Yielding supports (generally accepted as yielding steel arch) are able to accommodate certain rock deformations without being damaged. The ideal supporting curve for yielding supports is shown in Fig. 3. The deforming stage of

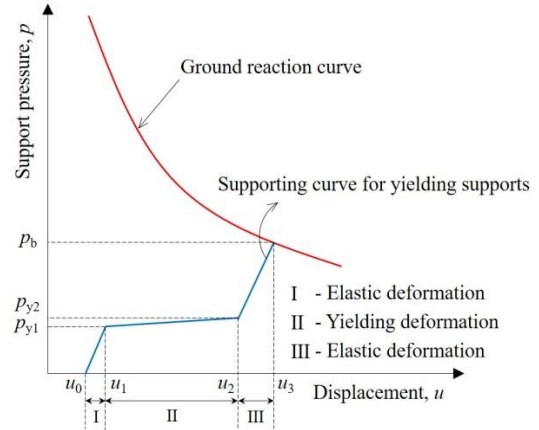


Fig. 3 Convergence-Confinement curve of tunnel using yielding supports

yielding supports before failure can be categorized as three stages: elastic deformation I, yielding deformation II and elastic deformation III (Wu *et al.* 2020). During yielding deformation phase, support pressure generally exhibits a slight increase as rock deformations greatly increase, which makes the yielding supports distinguished from the traditional stiff. It can be explained that in yielding steel arch, when the external pressure produces the necessary axial load the yielding steel arch starts its yielding phase. However, as the segments of the steel set slide, the friction surface (area of contact between the segments) increases and the necessary axial load should also increase (Brodny 2010). Therefore, the supporting curve shows a slope in yielding phase in Fig. 3. Rodríguez and Díaz-Aguado (2013) concluded that it is support stiffness that results in the different supporting characteristic curves in different stages, which can be measured using physical experiments. In this paper, based on the support stiffness in the elastic deformation I  $K_s$ , factors  $\lambda_1$  and  $\lambda_2$  are introduced to modify the support stiffnesses in the deformations II and III. In generally,  $\lambda_2$  can be considered to be equal to 1.

The supporting equations in these three stages can be expressed as follows

$$p_i = K_s \frac{u - u_0}{R_0} \quad (u_0 < u \leq u_1) \quad (12)$$

$$p_i = p_{y1} + \lambda_1 K_s \frac{u - u_1}{R_0} \quad (u_1 < u \leq u_2) \quad (13)$$

$$p_i = p_{y2} + \lambda_2 K_s \frac{u - u_2}{R_0} \quad (u_2 < u \leq u_3) \quad (14)$$

where  $p_i$  denotes the support pressure.  $u$  is the radial displacement in the rocks and support interface.  $p_{y1}$  and  $p_{y2}$  are support pressures for starting and finishing yielding deformation of supports, respectively.  $u_0$ ,  $u_1$  and  $u_2$  represent the tunnel displacement after tunnel excavation, displacements as supports start and finish yielding deformations, respectively.  $R_0$  is tunnel radius.

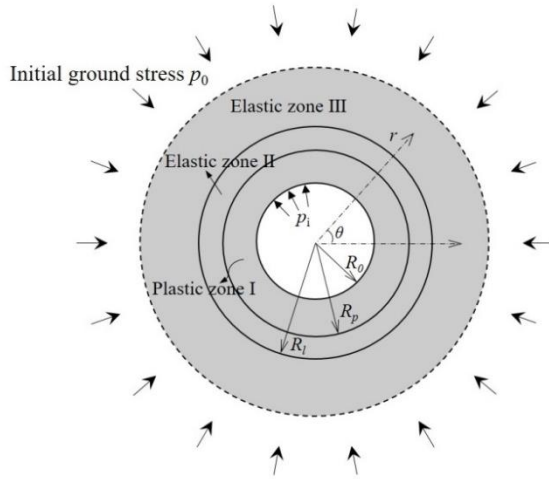


Fig. 4 Illustration for mechanical model of tunnel

For the stiff steel arch, there exists a calculation for stiffness, that is:  $K_s = E_s A_s / d \left( r_0 - \frac{h}{2} \right)$ , and  $E_s$  and  $A_s$  denote the Young's modulus for the steel and cross-sectional area of the arch, respectively.  $h$  is the height of the cross-section of the steel arch. For the stiffness in the first and third parts ( $\lambda_2=1$ ) of elastic deformations of yielding steel arch, the above formula can also be used. However, for the second part of yielding, the arch stiffness is associated with the axial force, which produces the yielding between arch segments and usually can be experimentally determined.

2.4 Tunnel behaviour prediction

The mechanical model of tunnels supported by rockbolts and yielding supports is shown in in Fig. 4. As accepted, the stress fields will not be influenced by rock parameters, but displacement fields are closely associated with these mechanical parameters. Based on the theory of elasticity, the stress fields in elastic zones II and III can be expressed as

$$\begin{cases} \sigma_r = p_0 \left( 1 - \frac{R_p^2}{r^2} \right) + \sigma_r^{(R_p)} \frac{R_p^2}{r^2} \\ \sigma_\theta = p_0 \left( 1 + \frac{R_p^2}{r^2} \right) - \sigma_r^{(R_p)} \frac{R_p^2}{r^2} \end{cases} \quad (15)$$

where  $p_0$  denotes the initial ground stress.  $R_p$  is the plastic radius in surrounding rocks.  $R$  represents the distance between tunnel center and element.  $\sigma_r^{(R_p)}$  is the radial stress at  $r=R_p$ .

Substituting  $r=R_p$  into the Eq. (15) gives

$$\sigma_\theta^{(R_p)} = 2p_0 - \sigma_r^{(R_p)} \quad (16)$$

In addition, Mohr-Coulomb strength criteria in polar coordinate system can also be expressed in the following format as

$$\frac{\sigma_\theta + a}{\sigma_r + a} = K \quad (17)$$

where

$$a = c^* \cot \varphi^* \quad (18)$$

and

$$K = \frac{1 + \sin \varphi^*}{1 - \sin \varphi^*} \quad (19)$$

By use of the Eqs. (16) and (17),  $\sigma_r^{(R_p)}$  and  $\sigma_\theta^{(R_p)}$  can be calculated as

$$\begin{cases} \sigma_r^{(R_p)} = \frac{2}{1+K} (p_0 + a) - a \\ \sigma_\theta^{(R_p)} = \frac{2K}{1+K} (p_0 + a) - a \end{cases} \quad (20)$$

For elastic zone II, it can be considered as a thick cylinder, the displacement of the inner and outer surfaces can be given by

$$u_r^{(R_p)} = \frac{1-\nu^{*2}}{E^* R_p} \left[ - \left( \frac{R_l^2 + R_p^2}{R_l^2 - R_p^2} + \frac{\nu^*}{1-\nu^*} \right) \sigma_r^{(R_p)} R_p^2 + \frac{2R_p^2 R_l^2 \sigma_r^{(R_l)}}{R_l^2 - R_p^2} \right] \quad (21)$$

$$u_r^{(R_l)} = \frac{1-\nu^{*2}}{E^* R_l} \left[ - \frac{2R_p^2 R_l^2 \sigma_r^{(R_p)}}{R_l^2 - R_p^2} + \left( \frac{R_l^2 + R_p^2}{R_l^2 - R_p^2} - \frac{\nu^*}{1-\nu^*} \right) \sigma_r^{(R_l)} R_l^2 \right] \quad (22)$$

where  $u_r^{(R_p)}$  and  $u_r^{(R_l)}$  denote the radial displacements in the plastic zone I /elastic zone II interface and elastic zone II /elastic zone III interface, respectively.  $R_l$  is length of rockbolts.  $\sigma_r^{(R_l)}$  represents the radial stress in the elastic zone II /elastic zone III interface.

For elastic zone III, due to the initial ground stress  $p_0$  at infinity and  $\sigma_r^{(R_l)}$  in the elastic zone II /elastic zone III interface, the radial displacement can be expressed as

$$u_r^{(R_l)} = \frac{R_l (1 + \nu_1)}{E_1} \left[ 2(1 - \nu_1) p_0 - \sigma_r^{(R_l)} \right] \quad (23)$$

Then, by use of the Eqs. (22) and (23),  $\sigma_r^{(R_l)}$  can be derived. As a consequence, substituting  $\sigma_r^{(R_l)}$  into the Eqs. (21) and (22) can yield  $u_r^{(R_p)}$  and  $u_r^{(R_l)}$ , respectively.

Actually, there exists an initial displacement due to the initial ground stress before tunnel excavation, which should be taken into account in the calculation. On account of no excavation, this elastic initial displacement can be expressed as

$$u = \frac{r(1 + \nu_1)(1 - 2\nu_1)}{E_1} p_0 \quad (24)$$

Therefore, the above displacements  $u_r^{(R_i)}$  and  $u_r^{(R_p)}$  obtained should cut down the elastic initial displacement, and the actual displacement induced by tunnel excavation can be rewritten as

$$\Delta u_r^{(R_i)} = u_r^{(R_i)} - u_r^{(R_i)} \quad (25)$$

$$\Delta u_r^{(R_p)} = u_r^{(R_p)} - u_r^{(R_p)} \quad (26)$$

In addition, equilibrium equation for plane problem of a circular tunnel in polar coordinate system can be written as

$$\frac{d\sigma_r}{dr} + \frac{\sigma_r - \sigma_\theta}{r} = 0 \quad (27)$$

At tunnel wall, namely,  $r = R_0$ ,  $\sigma_r^{(R_0)} = p_i$ . Combining the Eqs. (17) and (27), the stress filed in plastic zone can be calculated as

$$\begin{cases} \sigma_r = (p_i + a) \left(\frac{r}{R_0}\right)^{K-1} - a \\ \sigma_\theta = (p_i + a) K \left(\frac{r}{R_0}\right)^{K-1} - a \end{cases} \quad (28)$$

Substituting  $r = R_p$  into the Eq. (28) yields

$$\sigma_r^{(R_p)} = (p_i + a) \left(\frac{R_p}{R_0}\right)^{K-1} - a \quad (29)$$

The Eq. (20) also provides the radial stress in the plastic zone I/elastic zone II interface. By use of the Eqs. (20) and (29), the plastic radius can be calculated as

$$R_p = R_0 \left[ \frac{2}{1+K} \frac{(p_0 + a)}{p_i + a} \right]^{\frac{1}{K-1}} \quad (30)$$

where  $p_i$  denotes the interaction pressure between rocks and supports.

According to the theory of plasticity, when the shape of the rock and soil change due to plastic deformation, the rock volumetric strain is almost zero. Then, the following equation should be satisfied

$$\varepsilon_r + \varepsilon_\theta = 0 \quad (31)$$

And geometric equations in polar coordinate system can be given by

$$\begin{cases} \varepsilon_r = \frac{du}{dr} \\ \varepsilon_\theta = \frac{u}{r} \end{cases} \quad (32)$$

Combining the Eqs. (31) and (32), the governing equation for displacement in plastic zone can be given by

$$\frac{du_p}{dr} + \frac{u_p}{r} = 0 \quad (33)$$

where  $u_p$  represents the displacement in plastic zone.

In the Eq. (26),  $\Delta u_r^{(R_p)}$  has been provided; and using this boundary condition the Eq. (33) can be calculated as

$$u_p = \Delta u_r^{(R_p)} \frac{R_0}{r} \left[ \frac{2}{1+K} \frac{(p_0 + a)}{p_i + a} \right]^{\frac{1}{K-1}} \quad (34)$$

Because  $p_i$  is a variable related with rock displacement and there exists  $p_i$  in the Eqs. (25), (26) and (34), it is very difficult to give the accurate solutions for rock displacements and support pressure. In this paper, using Newton iterative method the rock displacements and support pressure can finally be determined.

### 3. Results and discussion

#### 3.1 Validation

In order to validate the theoretical analysis, a comparison between solutions in this paper and results in previous literature has been carried out. Because of some factors not being considered in previous study, in order to create the same calculating condition the support pressure equals to 1MPa. In addition, the initial ground stress, tunnel radius, rock parameters and rockbolt parameters are listed in Table 1, respectively.

As illustrated in Fig. 5, a comparison of rock displacement between solution in this paper and result in previous study has been performed. A good agreement between them shows the reliability and effectiveness of the theoretical analysis in this paper. From Fig. 5, rock displacement gradually decreases inward from the tunnel wall and the plastic radius of tunnel is 4.896 m.

#### 3.2 Parametric investigation

##### 3.2.1 Influence of rockbolt length

As generally accepted, rockbolt parameters are crucial for tunnel supporting effect. First, the investigation on the influence of rockbolt length is performed. In the calculation,

Table 1 Calculating parameters

Tunnel parameters			
Initial ground stress $p_0$ (MPa)	Radius $R_0$ (m)		
5	3		
Rock parameters			
Young's modulus $E_1$ (MPa)	Poisson's ratio $\nu_1$	Cohesion $c$ (kPa)	Internal friction angle $\varphi$ (°)
200	0.35	20	25
Rockbolt parameters			
Length $l$ (m)	Radius $R_b$ (mm)	Circumferential space $s_r$ (°)	Longitudinal space $s_z$ (m)
3	25	20	0.6

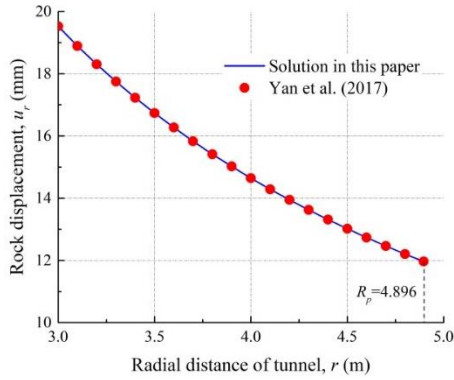


Fig. 5 Theoretical validation

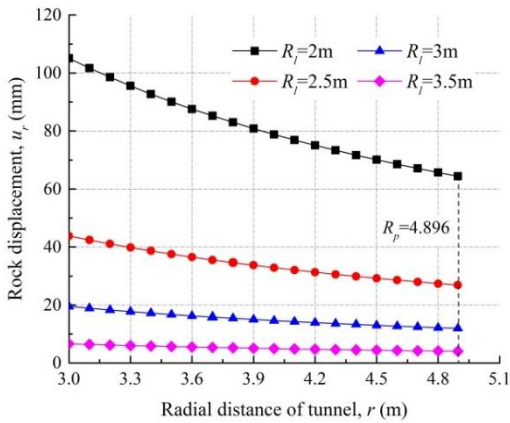


Fig. 6 Rock displacement along radial direction with different rockbolt lengths

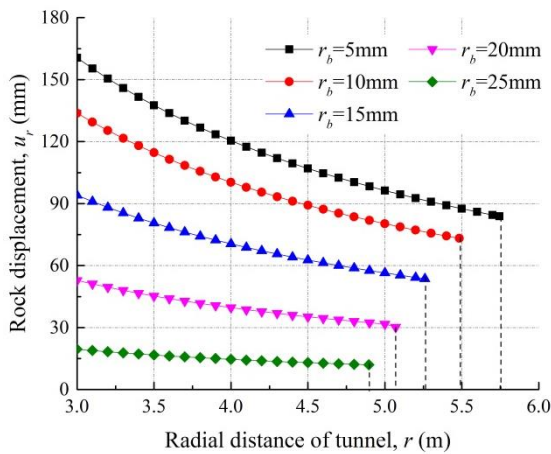


Fig. 7 Rock displacement along radial direction with different rockbolt radii

the initial ground stress, tunnel radius, rock parameters and support pressure are all taken from the above section. The radius of rockbolts is 25 mm, and circumferential space and longitudinal space are 20° and 1m, respectively. As shown in Fig. 6, curves for the rock displacement under the condition of different rockbolt lengths are plotted. These diagrams are drawn for  $R=2, 2.5, 3$  and  $3.5$  m.

Results in Fig. 6 clearly demonstrate that the rockbolt length has a great influence on rock displacement. From Fig. 6, the rock displacement at tunnel wall decreases from

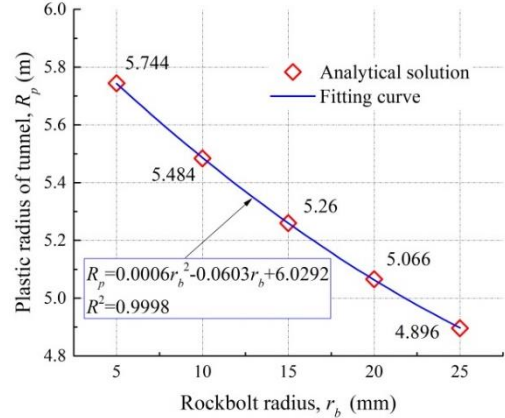


Fig. 8 Comparison of plastic radius of tunnel with different rockbolt radii

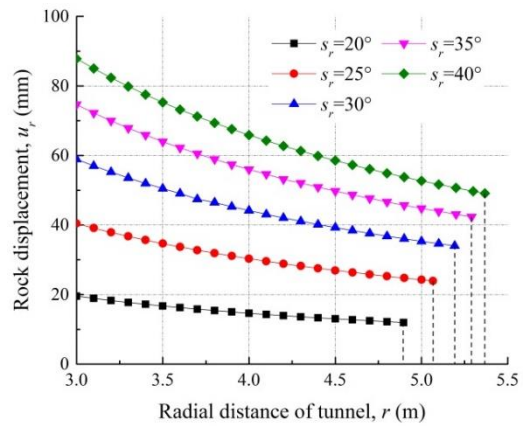


Fig. 9 Rock displacement along radial direction with different rockbolt circumferential spaces

105.12 mm to 43.86 mm when rockbolt length increases from 2 m to 2.5 m. Moreover, rock displacement continues to decrease as rockbolt length increases. It should be noted that if rockbolt length becomes large enough, the further improvement of rock displacement will not be obvious by still increasing their length. For instance, rock displacement only decreases from 19.53 mm to 6.62 mm as rockbolt length increases from 3 m to 3.5 m. Hence, it is safe to state that the installation of rockbolts in tunnels plays an important role in controlling rock displacement, and the effect on rock displacement reduction increases as the rockbolt length becomes larger. However, it is undesirable to further increase their length in order to achieve smaller rock displacement. For practical engineering, there should exist a reasonable length range for rockbolts.

In addition, it can be found from Fig. 6 that in spite of different rockbolt lengths the plastic radii of tunnel are equal in these cases. It can be explained that the reinforced zone is dominated by rockbolt length but mechanical parameters of the reinforced zone are controlled by their radius and installation density. That, the plastic radius of tunnel is the same in these four cases with same ground stress and support pressure.

### 3.2.2 Influence of rockbolt radius

The influence of rockbolt radius is then investigated.

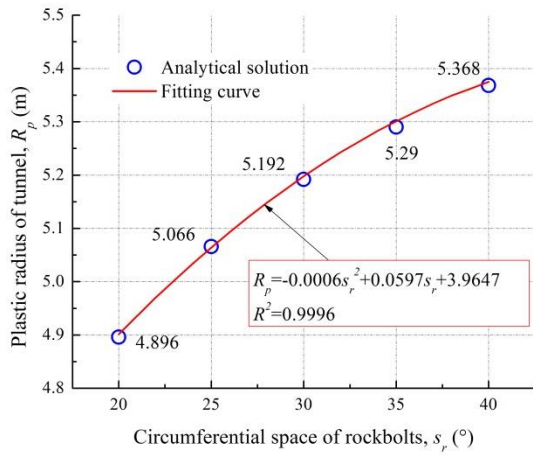


Fig. 10 Comparison of plastic radius of tunnel with different rockbolt circumferential spaces

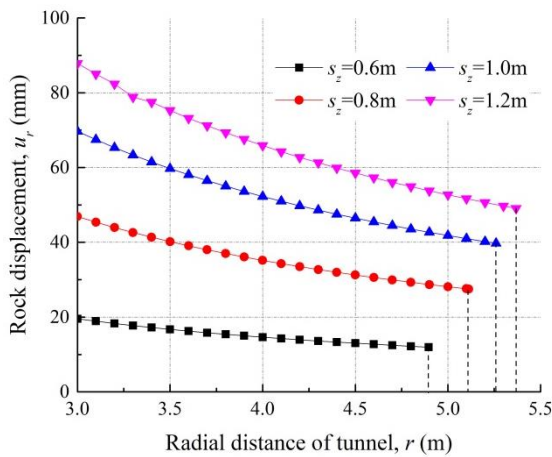


Fig. 11 Rock displacement along radial direction with different rockbolt longitudinal spaces

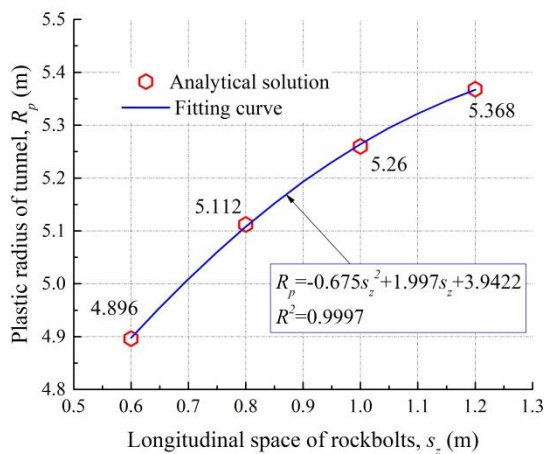


Fig. 12 Comparison of plastic radius of tunnel with different rockbolt longitudinal spaces

Under the condition of other parameters remaining constant, rockbolt length is determined as 3m, and radii are 5, 10, 15, 20 and 25 mm, respectively. As shown in Fig. 7, rockbolt radius significantly affects the rock displacement as well, and rock displacement decreases with the increase

of rockbolt radius. Interestingly, it can be found that the difference values of rock displacement at tunnel wall between two adjacent cases, for instance  $r_b=5$  mm and  $r_b=10$  mm, are 26.82, 39.74, 41.24 and 33.35 mm, respectively. This difference value increases first and then decreases although the value added of rockbolt radius is the same. It can be considered that in the condition of calculating parameters in this paper the utilization of rockbolts is the highest with the rockbolt radius of 20 mm. Therefore, the judgement that there is the highest utilization of rockbolts corresponding to a certain rockbolt radius can be made.

Fig. 8 shows the variation of plastic radius of tunnel with the rockbolt radius. It is clear from Fig. 8 that plastic radius of tunnel gradually decreases with the increase of rockbolt radius, and there exists a second order function relationship between the plastic radius of tunnel and rockbolt radius. Under the condition prescribed in this paper, the plastic radius of tunnel changes more quietly and the improvement is no longer evident.

### 3.2.3 Influence of rockbolt installation density (circumferential and longitudinal spaces)

It is generally accepted that more rockbolts need to be used in tunnels when excessive deformation occurs. The investigation on the effects of installation density of rockbolts including circumferential space and longitudinal space is conducted as well. In this analysis, the rockbolt length and radius are 3 m and 25 mm. As shown in Figs. 9 and 10, these curves for rock displacement and plastic radius of tunnel are plotted for circumferential spaces of rockbolts  $s_r=20^\circ$ ,  $25^\circ$ ,  $30^\circ$ ,  $35^\circ$  and  $40^\circ$ , respectively, and longitudinal space  $s_z$  of 0.6m. Curves in Figs. 9 and 10 are plotted with longitudinal spaces of rockbolts  $s_z = 0.6, 0.8, 1.0$  and  $1.2$  m, respectively, and circumferential space  $s_r$  of  $20^\circ$ .

Results in Figs. 9-12 show that the installation density of rockbolts plays an important role in controlling supporting effect. Rock displacement decreases with the reduction of either circumferential space or longitudinal space. Based on the results in Figs. 9 and 11, contrary to rockbolt length, the rock displacement decreases in an accelerative trend as either circumferential space or longitudinal space continues to decrease. For instance, rock displacement has dropped by 12.74 mm and 20.90 mm as circumferential space of rockbolts decreases from  $40^\circ$  to  $35^\circ$  and from  $25^\circ$  to  $20^\circ$ , respectively. It can also be found from Figs. 10 and 12 that the plastic radius of tunnel and rock displacement follow the same changing trend. Therefore, increasing the installation density of rockbolts is considered as an effective way to improve tunnel performance.

### 3.2.4 Influence of yielding displacement and stiffness parameter

For yielding supports, yielding displacement  $u_y$  and stiffness parameter for yielding  $\lambda_1$  are considered as the most important parameters. Here, the parametric investigations on these two parameters are also performed. The initial ground stress and tunnel radius remain

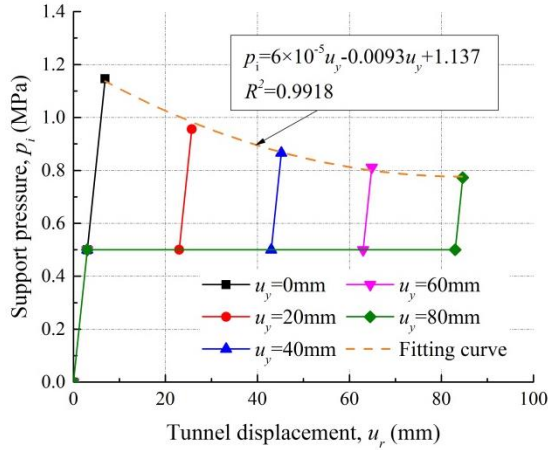


Fig. 13 Comparison of support pressure with different yielding displacements

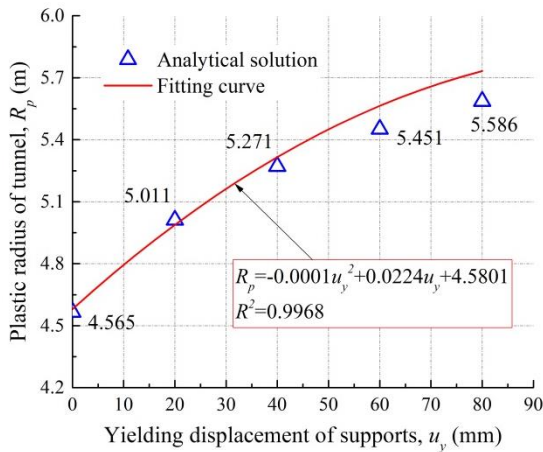


Fig. 14 Comparison of plastic radius of tunnel with different yielding displacements

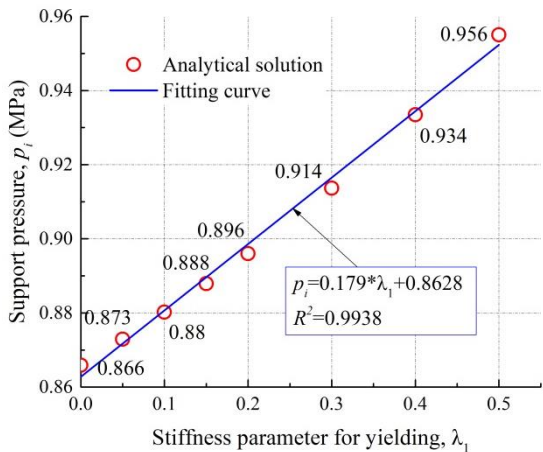


Fig. 15 Comparison of support pressure with different stiffness parameters for yielding  $\lambda_1$

unchanged. Rockbolt length, radius, circumferential space and longitudinal space are 3 m, 25 mm, 20° and 0.6m, respectively. The support stiffness is 500 MPa and the stiffness parameters for yielding  $\lambda_1$  and  $\lambda_2$  are 0 and 1. The support is considered to yield as support pressure reaches

0.5 MPa. As shown in Figs. 13 and 14, curves for support pressure and plastic radius of tunnel are presented with yielding displacement  $u_y=0, 20, 40, 60$  and  $80$  mm, respectively.

When the yielding displacement  $u_y$  is 0mm, yielding supports change to the traditional stiff supports. From Fig. 13, the supporting curve is a straight line in this condition and the support pressure reaches the maximum ( $p_i=1.15$  Mpa). With the increase of yielding displacement the support pressure gradually decreases. Similarly, a second order function relationship between support pressure and yielding displacement can be found in Fig. 13. When the yielding displacement exceeds 60 mm, the yielding effect becomes no longer obvious.

Fig. 14 provides the results of plastic radius of tunnel with different yielding displacements. Unfortunately, it can be seen that the plastic radius gradually increases because of greater yielding displacement causing smaller support pressure. Although this growing trend is slowing down, the aim of achieving smaller support pressure is in conflict with the control of plastic radius of tunnel by increasing yielding displacement. Actually, it deals with a complex process to determine an optimal yielding displacement and a comprehensive investigation is the prerequisite, combining rock properties, support characteristics and tunnel design requirements.

As shown in Fig. 15, this diagram is drawn for the stiffness parameters for yielding  $\lambda_1=0, 0.05, 0.1, 0.15, 0.2, 0.3, 0.4$  and  $0.5$ , respectively, and yielding displacement  $u_y=40$ mm. It can be seen from Fig. 15 that there exists a linear relationship between stiffness parameter for yielding  $\lambda_1$  and support pressure. In yielding deforming phase, the greater parameter  $\lambda_1$  of supports means the stronger restraint for rock deformation. When parameter  $\lambda_1=0$ , yielding supports can be referred as the completely yielding supports, and they change into the stiff with this parameter ranging from 0 to 1. However, considering the smaller support pressure resulting in larger plastic radius of tunnel, it is safe to conclude that it is better to choose completely yielding supports when other requirements for tunnel design are satisfied.

#### 4. Conclusions

Attempt has been proved to be effective that surrounding rock reinforcement is emphasized simultaneously considering displacement release in weak rock tunnels. The coupled influences of rockbolt reinforcement and yielding supports on tunnel mechanical response are analytically investigated. The calculation formulas for mechanical parameters of bolt-reinforced surrounding rock are first proposed using homogenization method; then then analytical solutions for rock displacement and support pressure around a circular bolt-reinforced and yielding supports-supported tunnel are provided. Finally, based on the analytical solutions a comprehensive parametric investigation is carried out. Some recommendations for the design of rockbolts and yielding supports can be obtained as follows:

Rockbolt length has a great influence on the rock displacement. The effect on rock displacement reduction gradually increases as the rockbolt length increases. However, when rockbolt length becomes large enough, the further improvement of rock displacement will not be obvious by still increasing their length. For rockbolt radius, both rock displacement and plastic zone of tunnel decrease with its increase. There should be the highest utilization of rockbolts corresponding to a certain rockbolt radius. In addition, the rock displacement and plastic zone of tunnel also decrease as installation density of rockbolts including circumferential space and longitudinal space increases. But under the condition prescribed, the decreasing trend changes more quietly and the improvement is no longer evident.

For yielding supports, yielding displacement and stiffness parameter for yielding in yielding deforming stage are the most important parameters. Larger yielding displacement and stiffness parameter lead to smaller support pressure, but greater plastic radius of tunnel. The optimal yielding displacement and stiffness parameters need to be determined through a comprehensive investigation combining rock properties, support characteristics and tunnel design requirements.

## Acknowledgments

The research described in this paper was financially supported by “National Natural Science Foundation of China” (No. 11872287), and “Found of Shaanxi Key Research and Development Program” (No. 2019ZDLGY01-10).

## References

- Barla, G., Bonini, M. and Semeraro, M. (2011), “Analysis of the behaviour of a yield-control support system in squeezing rock”, *Tunn. Undergr. Sp. Tech.*, **26**, 146-154. <https://doi.org/10.1016/j.tust.2010.08.001>.
- Bernaud, D., Buhan, P.D. and Maghous, S. (1995), “Numerical simulation of the convergence of a bolt-supported tunnel through a homogenization method”, *Int. J. Numer. Anal. Meth. Geomech.*, **19**, 267-288. <https://doi.org/10.1002/nag.1610190404>.
- Bobet, A. (2009), “Elastic solution for deep tunnels. Application to excavation damage zone and rockbolt support”, *Rock Mech. Rock Eng.*, **42**(2), 147-174. <https://doi.org/10.1007/s00603-007-0140-0>.
- Brichall, T.J. and Osman, A.S. (2012), “Response of a tunnel deeply embedded in a viscoelastic medium”, *Int. J. Numer. Anal. Met.*, **36**, 1717-1704. <https://doi.org/10.1002/nag.1069>.
- Brodny, J. (2010), “Determining the working characteristic of a friction joint in a yielding support”, *Arch. Min. Sci.*, **55**(4), 733-746.
- Cai, Y., Jiang, Y., Djamaluddin, I., Iura, T and Esaki, T. (2015), “An analytical model considering interaction behavior of grouted rock bolts for convergence-confinement method in tunneling design”, *Int. J. Rock Mech. Min. Sci.*, **76**, 112-126. <https://doi.org/10.1016/j.ijrmm.2015.03.006>.
- Cantieni, L. and Anagnostou, G. (2009), “The interaction between yielding supports and squeezing ground”, *Tunn. Undergr. Sp. Tech.*, **24**, 309-322. <https://doi.org/10.1016/j.tust.2008.10.001>.
- Chu, Z., Wu, Z., Liu, Q., Liu, B. and Sun, J. (2021a), “Analytical solution for lined circular tunnels in deep viscoelastic burgers rock considering the longitudinal discontinuous excavation and sequential installation of liners”, *J. Eng. Mech.*, **147**(4), 04021009. [https://doi.org/10.1061/\(ASCE\)EM.1943-7889.0001912](https://doi.org/10.1061/(ASCE)EM.1943-7889.0001912).
- Chu, Z., Wu, Z., Liu, Q., Weng, L., Wang, Z. and Zhou, Y. (2021b), “Evaluating the microstructure evolution behaviors of saturated sandstone using NMR testing under uniaxial short-term and creep compression”, *Rock Mech. Rock Eng.*, **54**, 1-23. <https://doi.org/10.1007/s00603-021-02538-4>.
- Cui, L., Zheng, J. Sheng, Q. and Pan, Y. (2019), “A simplified procedure for the interaction between fully-grouted bolts and rock mass for circular tunnels”, *Comput. Geotech.*, **106**, 177-192. <https://doi.org/10.1016/j.compgeo.2018.10.008>.
- Eftekhari, A. and Aalianvari, A. (2019). “An overview of several techniques employed to overcome squeezing in mechanized tunnels; A case study”, *Geomech. Eng.*, **18**(2), 215-224. <https://doi.org/10.12989/gae.2019.18.2.215>.
- Exadaktylos, G.E. and Stavropoulou, M.C. (2002) “A closed-form elastic solution for stresses and displacements around tunnels”, *Int. J. Rock Mech. Min. Sci.*, **39**(7), 905-916. [https://doi.org/10.1016/S1365-1609\(02\)00079-5](https://doi.org/10.1016/S1365-1609(02)00079-5).
- Fahimifar, A. and Ranjbarnia, M. (2009) “Analytical approach for the design of active grouted rockbolts in tunnel stability based on convergence-confinement method”, *Tunn. Undergr. Sp. Tech.*, **24**(4), 363-375. <https://doi.org/10.1016/j.tust.2008.10.005>.
- Fan, S., Song, Z., Zhang, Y. and Liu, N. (2020), “Case study of the effect of rainfall infiltration on a tunnel underlying the roadbed slope with weak inter-layer”, *KSCE J. Civ. Eng.*, **24**(5), 1607-1619. <https://doi.org/10.1007/s12205-020-1165-0>.
- Fan, S., Song, Z., Xu, T., Wang, K. and Zhang, Y. (2021), “Tunnel deformation and stress response under the bilateral foundation pit construction - a case study”, *Arch. Civ. Mech. Eng.*, **21**(3), 109. <https://doi.org/10.1007/s43452-021-00259-7>.
- Hoek, E. and Guevara, R. (2009), “Overcoming squeezing in the Yacambú-Quibor Tunnel, Venezuela”, *Rock Mech. Rock Eng.*, **42**(2), 389-418. <https://doi.org/10.1007/s00603-009-0175-5>.
- Indraratna, B. and Kaiser, P.K. (1990), “Analytical model for the design of grouted rock bolts”, *Int. J. Numer. Anal. Meth. Geomech.*, **14**(4), 227-251. <https://doi.org/10.1002/nag.1610140402>.
- Kargar, A.R., Rahmamejad, R. and Hajabasi, M.A. (2014), “A semi-analytical elastic solution for stress field of lined non-circular tunnels at great depth using complex variable method”, *Int. J. Solids Struct.*, **51**(6), 1475-1482. <https://doi.org/10.1016/j.ijsolstr.2013.12.038>.
- Kimura, F., Okabayashi, N and Kawamoto, T. (1987), “Tunnelling through squeezing rock in two large fault zones of the Enasan Tunnel II”, *Rock Mech. Rock Eng.*, **20**(3), 151-166.
- Moritz, B. (2011). “Yielding elements—requirements, overview and comparison/Stauchelemente”, *Geomech. Tunn.*, **4**(3), 221-236. <https://doi.org/10.1002/geot.201100014>.
- Osgoui, R.R., and Oreste, P. (2007), “Convergence-control approach for rock tunnels reinforced by grouted bolts, using the homogenization concept”, *Geotech. Geol. Eng.*, **25**(4), 431-440. <https://doi.org/10.1007/s10706-007-9120-0>.
- Öge, İ.F. (2021), “Revisiting the assessment of squeezing condition and energy absorption of flexible supports: A mine development case”, *Tunn. Undergr. Sp. Tech.*, **108**, 103712. <https://doi.org/10.1016/j.tust.2020.103712>.
- Radončić, N., Schubert, W. and Moritz, B. (2009), “Ductile support design”, *Geomech. Tunn.*, **5**, 561-577. <https://doi.org/10.1002/geot.200900054>.
- Ranjbarnia, M., Rahimpour, N. and Oreste, P. (2020), “A new analytical-numerical solution to analyze a circular tunnel using

- 3D Hoek-Brown failure criterion”, *Geomech. Eng.*, **22**(1), 11-23. <https://doi.org/10.12989/gae.2020.22.1.011>.
- Rodríguez, R. and Díaz-Aguado, M.B. (2013) “Deduction and use of an analytical expression for the characteristic curve of a support based on yielding steel ribs”, *Tunn. Undergr. Sp. Tech.*, **33**, 159-170. <https://doi.org/10.1016/j.tust.2012.07.006>.
- Sun, Y., Li, G., Zhang, J. (2020) “Investigation on jet grouting support strategy for controlling time-dependent deformation in the roadway”, *Energy Sci. Eng.*, **8**(6), 2151-2158. <https://doi.org/10.1002/ese3.654>.
- Sun, Y., Li, G., Zhang, N., Chang, Q., Xu, J., Zhang, J. (2021) “Development of ensemble learning models to evaluate the strength of coal-grout materials”, *Int. J. Min. Sci. Tech.*, **31**(2), 153-162. <https://doi.org/10.1016/j.ijmst.2020.09.002>.
- Tan, X., Chen, W. Liu, H. Chan, A.H.C. Tian, H., Meng, X., Wang, F and Deng, X. (2017) “A combined supporting system based on foamed concrete and U-shaped steel for underground coal mine roadways undergoing large deformations”, *Tunn. Undergr. Sp. Tech.*, **68**, 196-210. <https://doi.org/10.1016/j.tust.2017.05.023>.
- Wong, H., Subrin, D and Dias, D. (2006) “Convergence-confinement analysis of a bolt supported tunnel using the homogenization method”, *Can. Geotech. J.*, **43**(5), 462-483. <https://doi.org/10.1139/t06-016>.
- Wu, K. and Shao, Z. (2019a) “Study on the effect of flexible layer on support structures of tunnel excavated in viscoelastic rocks”, *J. Eng. Mech.*, **14** (10), 04019077. [https://doi.org/10.1061/\(ASCE\)EM.1943-7889.0001657](https://doi.org/10.1061/(ASCE)EM.1943-7889.0001657).
- Wu, K., Shao, Z. (2019b), “Visco-elastic analysis on the effect of flexible layer on mechanical behavior of tunnels”, *Int. J. Appl. Mech.*, **11**(3), 1950027. <https://doi.org/10.1142/S1758825119500273>.
- Wu, K., Shao, Z. and Qin, S. (2020a), “An analytical design method for ductile support structures in squeezing tunnels”, *Arch. Civ. Mech. Eng.*, **20**, 91. <https://doi.org/10.1007/s43452-020-00096-0>.
- Wu, K., Shao, Z., Qin, S., Zhao, N. and Hu, H. (2020b), “Analytical-based assessment of effect of highly deformable elements on tunnel lining within viscoelastic rocks”, *Int. J. Appl. Mech.*, **12**(3), 2050030. <https://doi.org/10.1142/S1758825120500301>.
- Wu, K., Shao, Z., Qin, S., Wei, W. and Chu, Z. (2021a), “A critical review on the performance of yielding supports in squeezing tunnels”, *Tunn. Undergr. Sp. Tech.*, **115**, 103815. <https://doi.org/10.1016/j.tust.2021.103815>.
- Wu, K., Shao, Z., Qin, S., Zhao, N. and Chu, Z. (2021b), “An improved non-linear creep model for rock applied to tunnel displacement prediction”, *Int. J. Appl. Mech.*, **13**, 9. <https://doi.org/10.1142/S1758825121500958>.
- Wu, K., Shao, Z., Sharifzadeh, M., Hong, S. and Qin, S. (2022a), “Analytical computation of support characteristic curve for circumferential yielding lining in tunnel design”, *J. Rock Mech. Geotech. Eng.*, **14**, 1-9.
- Wu, K., Shao, Z., Sharifzadeh, M., Chu, Z., Qin, S. (2022b) “Analytical approach to estimating the influence of shotcrete hardening property on tunnel response”, *J. Eng. Mech.*, In Press.
- Yan, Q., Li, S., Xie, C., Wang, M. and Ding, K. (2017) “Analytical solution for ground characteristic curve of composite rock mass reinforced by bolts in circular tunnels”, *Chin. J. Rock Mech. Eng.*, **36**(12), 3021-3027.
- Zhao, N., Shao, Z., Wu, K., Chu, Z. and Qin, S. (2021), “Time-dependent solutions for lined circular tunnels considering rockbolts reinforcement and face advancement effects”, *Int. J. Geomech.*, **21**(10), 04021179. [https://doi.org/10.1061/\(ASCE\)GM.1943-5622.0002130](https://doi.org/10.1061/(ASCE)GM.1943-5622.0002130).